Colloid Polym Sci 275:1046–1059 (1997)

ORIGINAL CONTRIBUTION

E. Piorkowska

Nonisothermal crystallization of polymers in samples of finite dimensions

2. Description of spherulitic pattern formation

Received: 5 August 1996
Accepted: 17 July 1997

Dr. E. Piorkowska (✉)
Centre of Molecular and
Macromolecular Studies
Polish Academy of Sciences
Siekiewicza 112
90-363 Lodz, Poland

Abstract The formation and final form of spherulite pattern in samples of finite thickness, strips and plates, are described by means of the conversion degree, the rate of formation of spherulitic interiors and the distributions of distances from spherulites centers to spherulites interiors. Two model crystallization processes are considered: crystallization with instantaneous nucleation and isokinetic crystallization. The influence of the instantaneous nucleation at sample boundaries on the spherulitic structure formation is also discussed. The master curve approach for the processes considered is proposed. The results in analytical forms are verified by computer simulation of spherulitic crystallization in two- and three-dimensional samples of finite thickness.

Key words Nonisothermal crystallization – isokinetic crystallization – instantaneous nucleation – confined samples

Introduction

In the preceding paper [1] the mathematical approach elaborated earlier [2–4] for description of spherulitic structure formation was applied for crystallization in confined samples. The formulas derived are applicable to isothermal as well as to nonisothermal crystallization. In order to apply those formulas, one has to know the dependencies of the nucleation rate and spherulite growth rate on time. In the case of nonisothermal crystallization the knowledge of the temperature change with time permits to recalculate the temperature dependencies of the spherulite growth rate. However, the existing theories of primary nucleation in polymers do not permit to predict exactly the nucleation process during nonisothermal crystallization based on isothermal data. In this paper, for the sake of demonstration of the influence of sample boundaries on the spherulitic structure formation, the two model crystallization processes inside a sample are considered: crystallization with instantaneous nucleation and isokinetic crystallization. Also the case of the instantaneous spherulite nucleation at samples boundaries is considered. The computer simulation of nonisothermal crystallization of polymer in samples of finite thickness was carried out to verify the correctness of the mathematical model applied.

Kinetics of crystallization

According to the derivations in the preceding paper [1] the local conversion degree, α, the local rate of the formation of spherulites interiors, g, and the components related to spherulites nucleated inside a sample and at sample boundaries, α_i, g_i and α_s, g_s, respectively, at distances s and $2h - s > s$ from both sample boundaries, at time t, can be expressed by the following formulas:

$$\alpha(t, s, 2h - s) = 1 - \exp[-E(t) + H_i(t, s) + H_i(t, 2h - s) - H_s(t, s) - H_s(t, 2h - s)] , \quad (1)$$

$$\alpha(t, s, 2h - s) = \alpha_i(t, s, 2h - s) + \alpha_s(t, s, 2h - s) \quad (2)$$

$$g(t, s, 2h - s)\,dt = g_i(t, s, 2h - s)\,dt + g_s(t, s, 2h - s)\,dt \quad (3)$$

$$g_i(t, s, 2h - s)\,dt = \exp[-E(t) + H_i(t, s) + H_i(t, 2h - s) - H_s(t, s) - H_s(t, 2h - s)]\frac{\partial}{\partial t}[E(t) - H_i(t, s) - H_i(t, 2h - s)]\,dt\,, \quad (4)$$

$$g_s(t, s, 2h - s)\,dt = \exp[-E(t) + H_i(t, s) + H_i(t, 2h - s) - H_s(t, s) - H_s(t, 2h - s)]\frac{\partial}{\partial t}[H_s(t, s) + H_s(t, 2h - s)]\,dt\,, \quad (5)$$

$$\alpha_i(t, s, 2h - s) = \int_0^t g_i(\tau, s, 2h - s)\,d\tau$$

and

$$\alpha_s(t, s, 2h - s) = \int_0^t g_s(\tau, s, 2h - s)\,d\tau\,, \quad (6)$$

where $2h$ denotes the sample thickness, and the functions E, H_i and H_s are listed below:

$$E(t) = v\pi \int_0^t F(\tau)\, r^n(\tau, t)\,d\tau\,, \quad (7)$$

where $v = 1$, $n = 2$ for a two-dimensional (2D) case, and $v = 4/3$, $n = 3$ for a three-dimensional (3D) case. $H_i(t, s)$ and $H_s(t, s)$ are nonzero functions for $s < r(0, t)$:

$$H_i^{(2)}(t, s) = \int_0^{t^*} F(\tau)\{\arctan\{[r^2(\tau, t)/s^2 - 1]^{0.5}\}r^2(\tau, t) - s[r^2(\tau, t) - s^2]^{0.5}\}\,d\tau\,, \quad (8a)$$

$$H_i^{(3)}(t, s) = (\pi/3)\int_0^{t^*} F(\tau)[s^3 + 2r^3(\tau, t) - 3r^2(\tau, t)\,s]\,d\tau\,, \quad (8b)$$

$$H_s^{(2)}(t, s) = 2\int_0^{t^*} F_s(\tau)[r^2(\tau, t) - s^2]^{0.5}\,d\tau\,, \quad (9a)$$

$$H_s^{(2)}(t, s) = \pi \int_\tau^{t^*} F_s(\tau)[r^2(\tau, t) - s^2]\,d\tau\,, \quad (9b)$$

where $r(\tau, t) = \int_\tau^t G(y)\,dy$, $G(t)$, $F(t)$ and $F_s(t)$ denote the time-dependent spherulite growth rate and nucleation rates, inside a polymer and at sample boundaries, respectively, t^* is defined by the relation: $r(t^*, t) = s$. The numbers in parentheses denote dimensionality. If nucleation occurs only inside a polymer i.e. $F_s = 0$, then $H_s = 0$. So $\alpha_s = 0$, $g_s = 0$, while $H = H_i$, $g = g_i$, $\alpha = \alpha_i$. The average functions for entire sample denoted by subscript "av": α_{av} α_{iav}, α_{sav}, g_{av} g_{iav} and g_{sav} are integrals of functions α, α_i, α_s, g, g_i and g_s over the range $0 < s < h$ divided by h.

Model modes of nucleation

The instantaneous mode (all spherulites start to grow at the same time) reflects the situation when the self-seeded nuclei are present in the melt and become all simultaneously active and it also describes the case of strong heterogeneous nucleation. The time dependence of the nucleation rate is then described as $F(t) = D\delta(t)$, where D denotes the number of nuclei per unit area (or volume) of a sample, and $\delta(t)$ is the Dirac delta function. The second crystallization mode considered, isokinetic crystallization during which the ratio of nucleation rate to spherulite growth rate remains constant, $F(t)/G(t) = P = \text{const.}$, serves as an example of the nucleation process prolonged with time. Crystallization without nucleation at sample boundaries as well as the process in which instantaneous nucleation at sample boundaries occurs with the density $F_s(t) = D_s\delta(t)$ is considered. The functions $H_i(t, s)$ for $s < r(0, t)$, and $E(t)$, are listed in Table 1 for 2D and 3D cases, for both considered crystallization processes inside a sample. For instantaneous nucleation at sample boundaries the function $H_s(t, s)$ is nonzero for $s < r(0, t)$:

$$H_s^{(2)}(t, s) = 2D_s[r^2(0, t) - s^2]^{0.5}$$

and

$$H_s^{(3)}(t, s) = D_s\pi[r^2(0, t) - s^2]\,. \quad (10)$$

The dependencies for confined samples for model nucleation processes differ from those describing similar relationships for infinite samples [3]. However, similarly as for infinite samples the kinetics of structure formation is determined by spherulite growth rate time dependence, $G(t)$, and also by the nucleation density, D, for instantaneous nucleation or the ratio of nucleation rate to spherulite growth rate, P, for isokinetic crystallization, respectively. In the presence of spherulitic nucleation at the sample boundaries also the nucleation density of that process, D_s, influences the structure formation. Locally, the formation of structure is influenced by the distances from sample boundaries, while for entire sample by the sample thickness.

Kinetic master curves

It should be noted here that all functions listed above (Table 1 and Eqs. (10)) can be easily expressed as functions of extended radius, R, defined as follows:

$$R = r(0, t) \quad \text{and} \quad dR = G(t)\,dt\,. \quad (11)$$

It was shown previously [3] for infinite samples that introduction of a new variable $u = r(0, t)/R_h$, where

Colloid & Polymer Science, Vol. 275, No. 11 (1997)

$R_h = r(0, t_h)$ and t_h is the half-time of crystallization, permits to present all relationships in a form characteristic for a type of process. For instantaneous nucleation R_h equals $[(\pi D)^{-1} \ln 2]^{0.5}$ and $[4(\pi D)^{-1} 3 \ln 2]^{1/3}$ in 2D and 3D cases, respectively. For isokinetic crystallization R_h equals $[3(\pi P)^{-1} \ln 2]^{1/3}$ and $[3(\pi P)^{-1} \ln 2]^{0.25}$ in 2D and 3D cases, respectively [3]. Here, introduction of a variable u accompanied by substitutions $y = s/R_h$ and $B = h/R_h$ results in the following forms of expressions for conversion degree, $\hat{\alpha}$, and the components of conversion rate, $\hat{g}_i$ and $\hat{g}_s$:

$$\hat{\alpha}(u, y, 2B - y) = 1 - 2^{-f(u)} \exp[H_{Bi}(u, y) + H_{Bi}(u, 2B - y) - H_{Bs}(u, y) - H_{Bs}(u, 2B - y)] \quad (12)$$

$$\hat{g}_i(u, y, 2B - y)\,du = 2^{-f(u)} \exp[H_{Bi}(u, y) + H_{Bi}(u, 2B - y) - H_{Bs}(u, y) - H_{Bs}(u, 2B - y)] \times \frac{\partial}{\partial u} [\ln(2) f(u) - H_{Bi}(u, y) - H_{Bi}(u, 2B - y)]\,du \quad (13)$$

$$\hat{g}_s(u, y, 2B - y)\,du = 2^{-f(u)} \exp[H_{Bi}(u, y) + H_{Bi}(u, 2B - y) - H_{Bs}(u, y) - H_{Bs}(u, 2B - y)] \times \frac{\partial}{\partial u} [H_{Bs}(u, y) + H_{Bs}(u, 2B - y)]\,du\,. \quad (14)$$

The conversion rate $\hat{g}$ is a sum of $\hat{g}_s$ and $\hat{g}_i$, while the components of conversion degree, $\hat{\alpha}_i$ and $\hat{\alpha}_s$, are integrals of $\hat{g}_s$ and $\hat{g}_i$ over the appropriate range of u. Functions $H_{Bi}(u, y)$ for $y < u$ and $f(u)$ for model processes inside a sample are listed in Table 1. $H_{Bi}(u, y)$ and $H_{Bs}(u, y)$ equal zero for $y > u$. For instantaneous nucleation at sample boundaries H_{Bs} function is nonzero for $u > y$:

$$H^{(2)}_{Bs}(u, y) = k \ln(2)(u^2 - y^2)^{0.5}$$

and

$$H^{(3)}_{Bs}(u, y) = k^2 \ln(2)(u^2 - y^2)\,, \quad (15)$$

where $k = R_h/R_{hs}$ and R_{hs} denotes the radius at conversion half-time at sample boundary, when process inside the sample is neglected:

$$R^{(2)}_{hs} = (2D_s)^{-1} \ln(2) \quad \text{and} \quad R^{(3)}_{hs} = [(\pi D_s)^{-1} \ln(2)]^{0.5}\,. \quad (16)$$

The average functions for entire sample, $\hat{\alpha}_{av}$, $\hat{\alpha}_{iav}$, $\hat{\alpha}_{sav}$, $\hat{g}_{av}$, $\hat{g}_{iav}$ and $\hat{g}_{sav}$ are integrals of respective local functions over the range $0 < y < B$ and divided by B. The average functions have different forms for the three ranges of u: $u < B$, $B < u < 2B$ and $2B < u$.

The relationships describing the formation of the spherulitic structure expressed as functions of the variable u are characteristic for the mode of nucleation and the sample dimensionality but depend also on the ratios of distances to sample boundary to R_h. The average functions depend on the ratio h/R_h. If additional nucleation process

Table 1 The E, H_i, f, H_{Bi}, E_C, H_{iC}, functions for two processes inside a sample: crystallization from instantaneous nuclei (IN) and isokinetic crystallization (IS)

Function	IN	IS
$E^{(2)}(t)$	$\pi D r^2(0, t)$	$(1/3)\pi P r^3(0, t)$
$H^{(2)}_i(t, s)$	$D\{r^2(0, t) \arctan\{[r^2(0, t)/s^2 - 1]^{0.5}\} - s[r^2(0, t) - s^2]^{0.5}\}$	$(P/3)\{r^3(0, t)\arctan\{[r^2(0, t)/s^2 - 1]^{0.5}\} + s^3\ln\{[r^2(0, t)/s^2 - 1]^{0.5} + r(0, t)/s\} - 2sr(0, t)[r^2(0, t) - s^2]^{0.5}\}$
$E^{(3)}(t)$	$(4/3)\pi D r^3(0, t)$	$(1/3)\pi P r^4(0, t)$
$H^3_i(t, s)$	$(D\pi/3)[s^3 + 2r^3(0, t) - 3r^2(0, t)s]$	$(P\pi/6)\,[r^2(0, t) - s^2][r(0, t) - s]^2$
$f^{(2)}(u)$	u^2	u^3
$H^{(2)}_{Bi}(u, y)$	$\pi^{-1} \ln(2)\{u^2 \arctan[(u^2/y^2 - 1)^{0.5}] - z(u^2 - y^2)^{0.5}\}$	$\pi^{-1}\ln(2)\{u^3 \arctan[(u^2/y^2 - 1)^{0.5}] + y^3\ln[(u^2/y^2 - 1)^{0.5} + u/y] - 2yu(u^2 - y^2)^{0.5}\}$
$f^{(3)}(u)$	u^3	u^4
$H^{(3)}_{Bi}(u, y)$	$0.25 \ln(2)(y^3 + 2u^3 - 3u^2 y)$	$0.5\ln(2)(u^2 - y^2)\,(u - y)^2$
$E^{(2)}_C(v)$	v^2	$[\Gamma(1/3)]^{-3/2} v^3$
$H^{(2)}_{iC}(v, x)$	$\pi^{-1}\{v^2 \arctan[(v^2/x^2 - 1)^{0.5}] - x(v^2 - x^2)^{0.5}\}$	$\pi^{-1}[\Gamma(1/3)]^{-3/2}\{v^3\arctan[(v^2/x^2 - 1)^{0.5}] + x^3\ln[(v^2/x^2 - 1)^{0.5} + v/x] - 2xv(v^2 - x^2)^{0.5}\}$
$E^{(3)}_C(v)$	v^3	$[\Gamma(1/4)]^{-4/3} v^4$
$H^{(3)}_{iC}(v, x)$	$0.25(x^3 + 2v^3 - 3xv^2)$	$0.5[\Gamma(1/4)]^{-4/3}(v^2 - x^2)(v - x)^2$

occurs at sample boundaries, the spherulitic structure formation is influenced also by the parameter k relating the extended radius at crystallization half-times for the crystallization process inside a polymer and at sample boundaries.

Distribution of distances from spherulites centers to spherulites inner points

The final spherulitic structure can be characterized by the distribution of distances, r, from spherulite centers to spherulites inner points. The distance distribution in a sample of thickness $2h$, according to ref. [1], is expressed by the following formula:

$$f_{av}(r, 2h)\,dr = f_{iav}(r, 2h)\,dr + f_{sav}(r, 2h)\,dr\,, \tag{17}$$

where functions f_i and f_s are the distributions of distances for spherulites nucleated inside a sample and for spherulites nucleated at sample surfaces, respectively, and are described by the equations:

$$f_{iav}(r, 2h)\,dr = h^{-1}\int_0^h [\Delta V(r) - \Delta S(r, s) - \Delta S(r, 2h - s)] \times f_i(r, s, 2h - s)\,ds \tag{18}$$

$$f_{sav}(r, 2h)\,dr = h^{-1}\int_0^h [\Delta L(r, s) + \Delta L(r, 2h - s)] \times f_s(r, s, 2h - s)\,ds \tag{19}$$

where

$$\Delta V^{(2)}(r) = 2\pi r\,dr \quad \text{and} \quad \Delta V^{(3)}(r) = 4\pi r^2\,dr\,. \tag{20}$$

The functions $\Delta S(r, s)$ and $\Delta L(r, s)$ are nonzero functions for $r > s$:

$$\Delta S^{(2)}(r, s) = 2r \arctan[(r^2/s^2 - 1)^{0.5}]\,dr$$

and

$$\Delta S^{(3)}(r, s) = 2\pi r(r - s)\,dr\,, \tag{21}$$

$$\Delta L^{(2)}(r, s) = 2r(r^2 - s^2)^{-0.5}\,dr \quad \text{and} \quad \Delta L^{(3)}(r, s) = 2\pi r\,dr\,. \tag{22}$$

The functions f_i and f_s for model crystallization from instantaneous nuclei and for isokinetic crystallization inside a sample take the forms

$$f_i(r, s, 2h - s) = D \exp[-E_N(r) + H_{iN}(r, s) + H_{iN}(r, 2h - s) - H_{sN}(r, s) - H_{sN}(r, 2h - s)]\,, \tag{23}$$

$$f_i(r, s, 2h - s) = P\int_r^\infty \exp[-E_N(z) + H_{iN}(z, s) + H_{iN}(z, 2h - s) - H_{sN}(z, s) - H_{sN}(z, 2h - s)]\,dz\,, \tag{24}$$

where $E_N(r)$, $H_{iN}(r, s)$ and $H_{sN}(r, s)$ functions are obtained by substitution $r = r(0, t)$ to functions E, H_i and H_s (Table 1 and Eqs. (10)). It should be noted that if the primary nucleation occurs only inside a sample then $f_s(r, s, 2h - s)$ and $H_{sN}(r, s)$ equal zero. For instantaneous nucleation at sample boundaries the function f_s is nonzero and has the form

$$f_s(r, s, 2h - s) = D_s \exp[-E_N(r) + H_{iN}(r, s) + H_{iN}(r, 2h - s) - H_{sN}(r, s) - H_{sN}(r, 2h - s)]\,. \tag{25}$$

f_{iav} and f_{sav} expressed by Eqs. (18)–(22) are in different forms for the three ranges of distance r: $r < h$, $h < r < 2h$ and $2h < r$. From Eqs. (23)–(25) it follows that the final spherulitic structure is determined by the sample thickness and the density of nucleation, D, for crystallization with instantaneous nucleation or by the ratio of nucleation rate to spherulite growth rate, P, for the isokinetic process. For additional instantaneous nucleation at sample boundaries, also the nucleation density D_s influences the spherulitic structure.

Similarly as for the case of crystallization in infinite samples [4] introduction of a new variable, $v = r/r_s$, where r_s is a radius of average spherulite in infinite sample, permits to express the distance distributions for model processes considered in a form characteristic for the crystallization mode. The radii of average spherulites, r_s, are related to the numbers of spherulites per area or volume unit, N: $r_s^{(2)} = (\pi N)^{-0.5}$ and $r_s^{(3)} = (4\pi N/3)^{-1/3}$. For instantaneous nucleation N equals D, while for isokinetic crystallization N equals $\pi^{1/3}(P/3)^{2/3}\Gamma(1/3)$ and $0.75\pi^{0.25}(P/3)^{0.75}\Gamma(1/4)$ for 2D and 3D cases, respectively. The relationships (18) and (19) assume the following forms for crystallization from instantaneous nuclei:

$$\hat{f}_{iav}(v, 2C)\,dv = C^{-1}\int_0^C \frac{\partial}{\partial v}[E_C(v) - H_{iC}(v, x) - H_{iC}(v, 2C - x)] \times \exp[-E_C(v) + H_{iC}(v, x) + H_{iC}(v, 2C - x) - H_{sC}(v, x) - H_{sC}(v, 2C - x)]\,dx\,dv \tag{26}$$

and for isokinetic crystallization,

$$\hat{f}_{iav}(v, 2C)\,dv = C^{-1}\int_0^C \frac{\partial^2}{\partial v^2}[E_C(v) - H_{iC}(v, x) - H_{iC}(v, 2C - x)] \times \int_v^\infty \exp[-E_C(w) + H_{iC}(w, x) + H_{iC}(w, 2C - x) - H_{sC}(w, x) - H_{sC}(w, 2C - x)]\,dw\,dx\,dv\,, \tag{27}$$

where $x = s/r_s$ and $C = h/r_s$ and $H_C(v, x)$ is nonzero for $v > x$. The functions $H_{iC}(v, x)$ for $v > x$ and $E_C(v)$ are listed in Table 1. For instantaneous nucleation at sample

Colloid & Polymer Science, Vol. 275, No. 11 (1997)

boundaries $\hat{f}_s$ are the nonzero functions for $v > x$:

$$\hat{f}_{sav}(v, 2C)\,dv = C^{-1}\int_0^C \frac{\partial}{\partial v}[H_{sC}(v, x) + H_{sC}(v, 2C - x)] \times \exp[-E_C(v) + H_{iC}(v, x) + H_{iC}(v, 2C - x) - H_{sC}(v, x) - H_{sC}(v, 2C - x)]\,dx\,dv\,, \quad (28)$$

where $H_{sC}(v, x)$ is nonzero for $v > x$:

$$H_{sC}^{(2)}(v, x) = k_r(v^2 - x^2)^{0.5} \quad \text{and} \quad H_{sC}^{(3)}(v, x) = k_r^2(v^2 - x^2)\,, \quad (29)$$

where $k_r = r_s/r_{ss}$ and r_{ss} denotes the radius of average spherulite at a sample boundary if nucleation process inside a sample is neglected, equal to $(2D_s)^{-1}$ and to $(\pi D_s)^{-1/2}$ for a line and a plane, respectively. Equations (27)–(29) assume different forms for the three ranges of v: $v < C$, $C < v < 2C$ and $2C < v$. It should be noted, that the distributions of distances, r, derived above for crystallization from instantaneous nuclei have the same form as the expressions for conversion degree as a function of $r(0, t)$, so the distributions of distances $v = r/r_s$ could be obtained from the conversion rate by substituting $u = vr_s/R_{hs}$ to $\hat{g}(u)\,du$.

Number of spherulites

In samples where instantaneous nucleation occurs the final number of spherulites in a volume unit equals the density of primary nucleation. However, if the primary nucleation is prolonged in time, as for the case of isokinetic crystallization, the final number of spherulites depends on the way in which the conversion degree depends on time. Hence, the number of spherulites nucleated inside a sample in a volume unit during isokinetic crystallization at the distances s and $2h - s$ from sample boundaries, $N_i(s, 2h - s)$, and the average number of spherulites per sample volume unit, $N_{iav}(2h)$, are expressed in the following way:

$$N_i(s, 2h - s) = P\int_0^\infty [1 - \alpha_N(R, s, 2h - s)]\,dR\,, \quad (30)$$

$$N_{iav}(2h) = P\int_0^\infty [1 - \alpha_{Nav}(R, 2h)]\,dR\,, \quad (31)$$

where α_N and α_{Nav} denote the conversion degrees: local at distances s and $2h - s$ from sample boundaries and average over the sample, respectively, expressed as functions of extended radius, $R = r(0, t)$. Hence, also the radius of average spherulite differs from that for infinite sample.

Determination of parameters for master curves

The kinetics of spherulitic crystallization in entire sample depends on the relation between the spherulite extended radius, $r(0, t)$, and sample thickness, $2h$. Crystallization always starts in the range $u < B$ but ends in the range $u < B$, $B < u < 2B$ or $u > 2B$ depending on sample thickness and on spherulite extended radius at the end of crystallization. The extended radius is the maximum possible distance from any spherulite center to any point of that spherulite, hence it determines also the forms of Eqs. (26)–(28) describing the distribution of distances from spherulite centers to spherulites interiors. For the crystallization kinetics expressed in terms of variable $u = r(0, t)/R_h$ and for distance distributions as functions of variable $v = r/r_s$, the relationships between u and the parameter $B = h/R_h$, and between v and the parameter $C = h/r_s$, are decisive.

In order to estimate the differences in crystallization the confined samples practically ending the crystallization (0.99 conversion degree) in all three ranges of u were compared. The conversion degree in infinite samples equals $1-2^{-f(u)}$, where the forms of the function $f(u)$ are listed in Table 1 for instantaneous nucleation and isokinetic crystallization, respectively. Assuming $\alpha(u_e) = 0.99$, one obtains the following values of u_e: 2.58 for instantaneous nucleation in 2D sample, 1.88 for instantaneous nucleation in 3D sample and for isokinetic crystallization in 2D sample and 1.61 for isokinetic crystallization in 3D sample. According to those values and regarding possible differences in crystallization of samples of limited thickness the three values of parameter B: B_1, B_2 and B_3 were chosen for each model process in sample interior, fulfilling the conditions:

$$u_e < B_1, \quad B_2 < u_e < 2B_2, \quad u_e > 2B_3\,. \quad (32)$$

For B_1 the entire crystallization process occurs in the range $u < B_1$. For B_2 crystallization ends in the range $B_2 < u < 2B_2$, while for B_3 crystallization ends in the range $u > 2B_3$. The expressions for r_s and R_h permit to calculate the respective values of parameter C: C_1, C_2 and C_3 fulfilling the conditions:

$$v_e < C_1, \quad C_2 < v_e < 2C_2, \quad v_e > 2C_3\,. \quad (33)$$

Parameters B_1, B_2, B_3 and the respective C_1, C_2, C_3 for each crystallization process considered for sample interior are listed in Table 2. For C_1 only the range $v < C_1$ has to be considered. For C_2 also the range $C_2 < v < 2C_2$ has to be taken into account, while for C_3 all the three ranges of v have to be regarded.

For crystallization with additional instantaneous nucleation at sample boundaries $k = 1$ was assumed which

means equality of conversion half-times for processes in sample interior and at sample surfaces, if considered separately. The respective values of k_r parameters for distance distributions calculations were 0.83 and 0.95 for instantaneous nucleation inside 2D and 3D samples, respectively, 0.48 and 0.59 for isokinetic crystallization in 2D and 3D samples, respectively. For instantaneous nucleation inside a plate the crystallization processes for various values of parameter k will be considered in order to investigate the effect of increasing nucleation density at sample boundaries. For each B and k parameters, the conversion rate, the conversion degree, the distribution of distances from spherulites centers to spherulites internal points and also the components resulting from spherulites nucleated inside a polymer and at sample boundaries were calculated.

Computer simulation

In order to verify the analytical expressions a computer simulation of spherulitic crystallization in samples of finite thickness was performed for model crystallization processes: crystallization with instantaneous nucleation and isokinetic crystallization inside a sample characterized by parameters B_1 and B_3. For crystallization from instantaneous nuclei in a plate, also the process with instantaneous nucleation at sample boundaries ($k = 1$) was simulated. The computer simulation employed here was similar to that described in the detail by Piorkowska and Galeski [5], and Piorkowska [3]. Samples in forms of strips (2D) and plates (3D) of thickness of 40 units were simulated. The length of 2D samples or the length and depth of 3D samples varied from 100 to 1000 units depending on nucleation intensity in order to ensure the final number of spherulites exceeding 1000. The positions of spherulites centers were randomized by means of a pseudorandom number generator. It was assumed that the spherulite growth rate depends on time similarly as in RAPRA isotactic polypropylene [3, 6, 7] during cooling at the rate $a = 10°$/min assuming that 1 distance unit equals 1 μm:

$$G(t) = g_0 \exp\{-U[R(T - T_\infty)]^{-1}\} \times \exp\{-K_g[T(T_m^0 - T)]^{-1}\} \quad (34)$$

where $T(t) = T_0 - at$ and $g_0 = 8009\,\mathrm{cm\,s^{-1}}$, $U = 1500\,\mathrm{cal\,mol^{-1}}$, $K_g = 358\,400\,K^2$, $T_\infty = 231.2\,\mathrm{K}$ and $T_m^0 = 458.2\,\mathrm{K}$. Similarly as in ref. [3], T_0 assumed for computations was 132 °C. For the case of instantaneous nucleation all centers were created simultaneously at the beginning of the process. For the case of isokinetic crystallization the coordinates of primary nuclei were generated in 1 s time intervals. The nuclei located in already crystallized regions, i.e. occupied at least by one spherulite, were rejected. Each nucleation step was followed by the growth step–appropriate increase of spherulite radii according to Eq. (34). The nucleation and growth steps were repeated until no uncrystallized fraction of a sample was found for location of new spherulite nuclei. The number of spherulite centers for the process with instantaneous nucleation was equal DV where D is the nucleation density and V denotes the sample area or volume. The number of primary nuclei generated in each step for isokinetic process was equal to $PG(t)\,\Delta t V$, assuming $\Delta t = 1$ s, where $G(t)$ is described by Eq. (34), and P is the ratio of nucleation rate to spherulite growth rate. The values of D and P used for the determination of number of nuclei were calculated from parameters B_1 and B_3 on the basis of relationships between R_{hs} and D or P and are listed in Table 2. The values of D_s for the crystallization from instantaneous nuclei in a plate calculated from D values and $k = 1$ are listed in Table 3. For higher values of k the nucleation densities are equal to $k^2 D_s$, where D_s is calculated for $k = 1$. The time distributions of the formation of spherulite inner points, the time dependencies of the conversion degree and the distributions of distances from spherulite centers to spherulites inner points were determined by generation of 40 000 points at randomized positions followed by the calculations of the time of occlusion of each point by the first arriving spherulite and the distance from the point to that spherulite center.

The evolution of spherulites was visualized on a chosen cross-sectional plane.

Table 2 The parameters B and C assumed for calculations based on analytical expressions for crystallization with instantaneous nucleation (IN) and isokinetic crystallization (IS) together with the values of nucleation density, D, and the ratio of nucleation rate to spherulite growth rate, P, for computer simulation of samples of thickness of 40 units

Crystallization	B	C	P, D
IN, 2D sample	$B_1 = 6.30$	$C_1 = 5.24$	$D = 2.19 \times 10^{-2}$
	$B_2 = 1.85$	$C_2 = 1.54$	—
	$B_3 = 1.06$	$C_3 = 0.88$	$D = 6.25 \times 10^{-4}$
IS, 2D sample	$B_1 = 4.59$	$C_1 = 6.65$	$P = 8.0 \times 10^{-3}$
	$B_2 = 1.34$	$C_2 = 1.94$	—
	$B_3 = 0.78$	$C_3 = 1.13$	$P = 3.9 \times 10^{-5}$
IN, 3D sample	$B_1 = 4.59$	$C_1 = 4.06$	$D = 2.0 \times 10^{-3}$
	$B_2 = 1.34$	$C_2 = 1.19$	—
	$B_3 = 0.78$	$C_3 = 0.69$	$D = 9.7 \times 10^{-6}$
IS, 3D sample	$B_1 = 3.92$	$C_1 = 5.50$	$P = 9.8 \times 10^{-4}$
	$B_2 = 1.15$	$C_2 = 1.61$	—
	$B_3 = 0.67$	$C_3 = 0.93$	$P = 8.1 \times 10^{-7}$

Table 3 The final numbers of spherulites per area or volume unit of a sample, per length or area unit of a sample boundary, and the radii of average spherulites: N and r_s for samples of infinite thickness, N_{iav} and r_{si}, for spherulites nucleated inside a sample of thickness of 40 units, D_s and r_{sb} for spherulites nucleated at boundaries. All values are listed for crystallization with instantaneous nucleation (IN) and isokinetic crystallization (IS) in 2D and 3D samples for k equal 0 and 1. The values of B_1 and B_3 are listed in Table 2

B	N	r_s	$k=0$		$k=1$			
			N_{iav}	r_{si}	N_{iav}	r_{si}	D_s	r_{sb}
IN, 2D								
B_1	2.19×10^{-2}	3.82	2.19×10^{-2}	3.82	2.19×10^{-2}	3.64	0.11	2.39
B_3	6.25×10^{-4}	22.57	6.25×10^{-4}	22.57	6.25×10^{-4}	16.20	1.84×10^{-2}	12.94
IN, 3D								
B_1	0.20×10^{-2}	4.92	0.20×10^{-2}	4.92	0.20×10^{-2}	4.75	1.16×10^{-2}	3.51
B_3	9.70×10^{-6}	29.09	9.70×10^{-6}	29.09	9.70×10^{-6}	22.49	3.33×10^{-4}	19.76
IS, 2D								
B_1	3.52×10^{-2}	3.01	3.58×10^{-2}	2.98	3.39×10^{-2}	2.90	0.79×10^{-1}	2.87
B_3	1.01×10^{-3}	17.74	1.13×10^{-3}	16.80	8.13×10^{-4}	13.46	1.35×10^{-2}	15.93
IS, 3D								
B_1	4.96×10^{-3}	3.64	5.03×10^{-3}	3.62	4.83×10^{-3}	3.54	8.49×10^{-3}	3.93
B_3	2.42×10^{-5}	21.45	2.62×10^{-5}	20.89	2.06×10^{-5}	17.34	2.44×10^{-4}	22.10

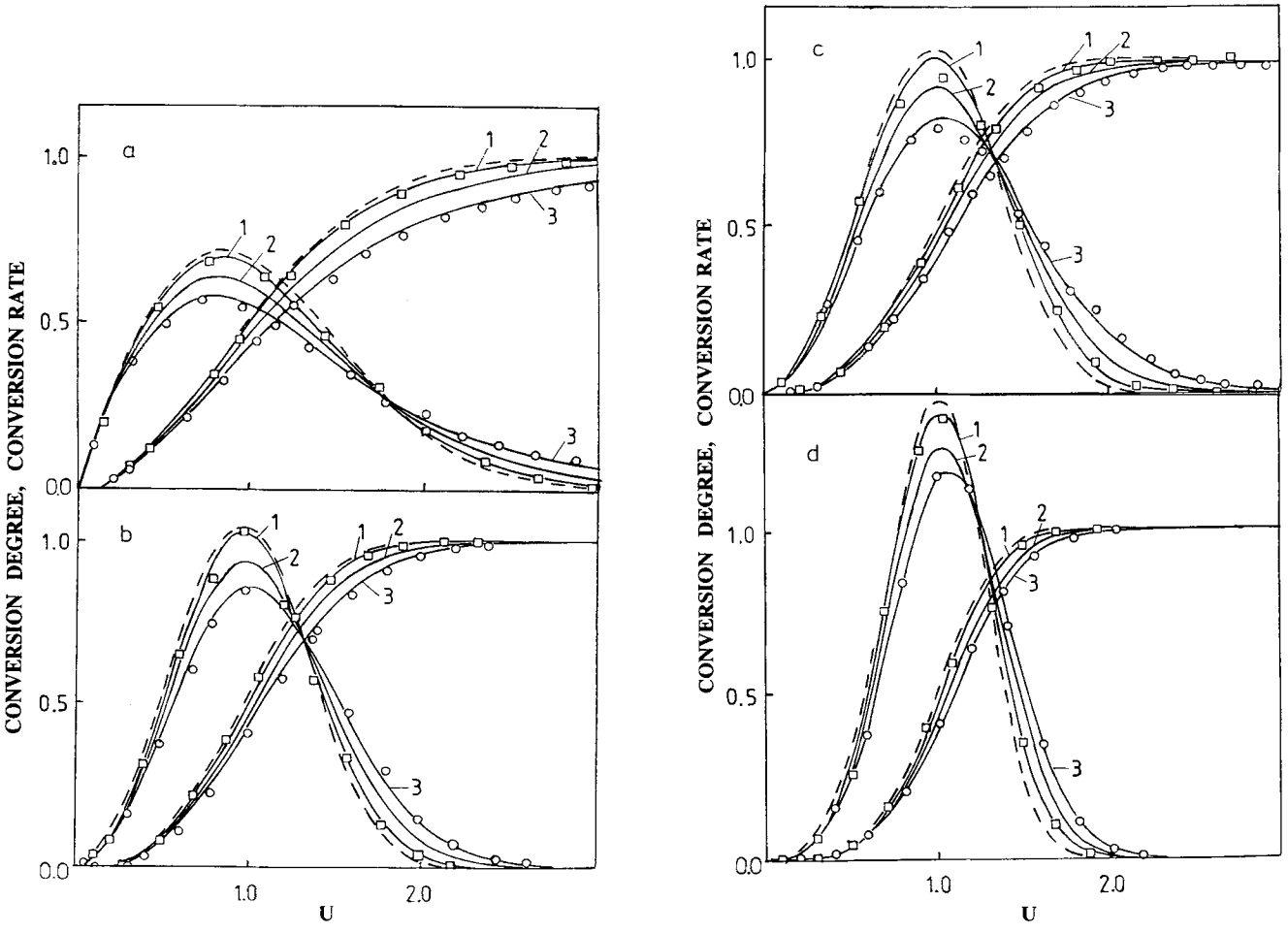

Fig. 1 The average conversion degrees and the average rates of conversion of melt into spherulites as functions of a variable $u = r(0, t)/R_h$ where $r(0, t)$ and R_h denote the "extended radius" at time t and at half-time of crystallization, respectively, for infinite samples (– – –) and for samples of finite thickness without nucleation at sample boundary (——) for parameters B_1 (curves #1), B_2 (curves #2) and B_3 (curves #3) from Table 2; a – 2D sample, instantaneous nucleation, b – 2D sample, isokinetic crystallization, c – 3D sample, instantaneous nucleation, d – 3D sample, isokinetic crystallization. Symbols denote the data from indedpendent computer simulation

Results

The average conversion degree and the average rate of spherulite interiors formation as functions of u for the instantaneous nucleation process and for the isokinetic crystallization in strips and plates, calculated on the basis of analytical expressions are plotted in Figs. 1a–d. For comparison the respective curves for infinite samples from ref. [3] are also plotted in Figs. 1a–d. The results of computer simulation, shown as symbols, follow theoretically obtained curves and indicate good agreement between computer simulation and the analytical dependencies. The kinetics of crystallization in samples of limited thickness differ from that in infinite samples. The differences are the smallest if the entire crystallization process occurs in the range of $u < B$, they are more pronounced for crystallization ending in the range $B < u < 2B$ and the most significant if crystallization is completed in the range $u > 2B$. It should be noted that the decrease of parameter B denotes either the decrease of sample thickness or the decrease of nucleation density. The examples of cross sections of plates with computer simulated crystallization from instantaneous nuclei characterized by parameters B_1 and B_3 are drawn in Fig. 2 for $u = 1$ and after a completion of crystallization. The smaller value of B the more pronounced influence of sample boundary and the slower crystallization process. In all cases considered the effect is very small at the beginning of crystallization but increases as the crystallization proceeds and it is best seen near the end of crystallization. For the cases considered, the value of u for which conversion degree equals 0.5 is shifted from 1 (infinite sample) to 1.1. The curves illustrating the formation of spherulite interiors, i.e. the first derivatives of the conversion degrees (see Fig. 1), are lower, broader and more slowly approaching zero than the curves for infinite samples. Except for the processes with instantaneous nucleation in 2D sample, also the slight shift of maximum towards larger values of u is visible.

In Figs. 3a–d the conversion degrees and rates of the formation of spherulites interiors as functions of variable u are plotted for crystallization processes with additional instantaneous nucleation on sample boundaries for B_1 and B_3 and $k = 1$. For all cases considered the additional nucleation process at sample boundaries causes the shortening of crystallization time, more significant for smaller values of B. In Figs. 3a–d also the component conversion degrees and the rates of the formation of spherulites interiors are plotted, separately for spherulites nucleated inside a sample and spherulites nucleated at sample boundaries. The symbols denote the results of computer simulation being in very good agreement with the analytically obtained curves. One can notice that the growth of both spherulite populations requires similar

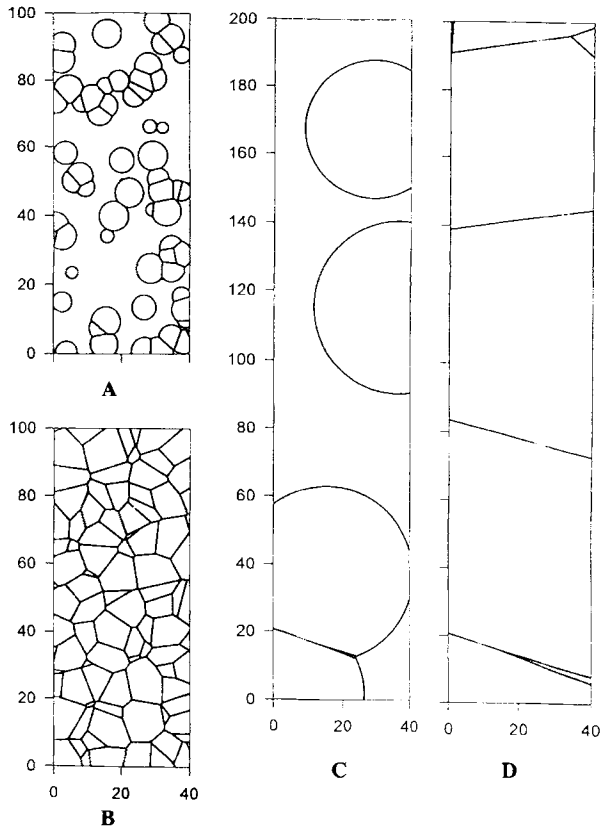

Fig. 2 The cross sections of spherulitic structures formed in a plate from instantaneous nuclei: during crystallization for $u = 1$ and after completion of crystallization, for parameters B_1 and B_3: a – B_1, $u = 1$, b – B_1, final structure, c – B_3, $u = 1$, d – B_3, final structure

period of time. It is seen that the influence of the nucleation at sample boundaries is stronger for the parameter B_3 than for B_1 (both listed in Table 2). Also the volume occupied by spherulites nucleated at sample boundaries increases from approximately 10% to 50% of sample volume.

In Figs. 4a–d the conversion degree dependencies on variable u are plotted for the sample boundary and for the middle of the sample for processes characterized by parameters B_3 and B_1 in the absence of nucleation at sample boundaries and for instantaneous nucleation at sample boundaries for $k = 1$. For B_1 the crystallization in the middle of sample proceeds as in an infinite sample while at sample boundary it is slower if no additional nucleation process occurs there. The instantaneous nucleation at sample boundary accelerates the conversion at sample boundary but has no influence on crystallization in the middle of the sample. The decrease of parameter B to B_3 results in slight changes of the conversion degree at sample boundary; the delay in the absence of nucleation at the boundary or acceleration if such process occurs, are

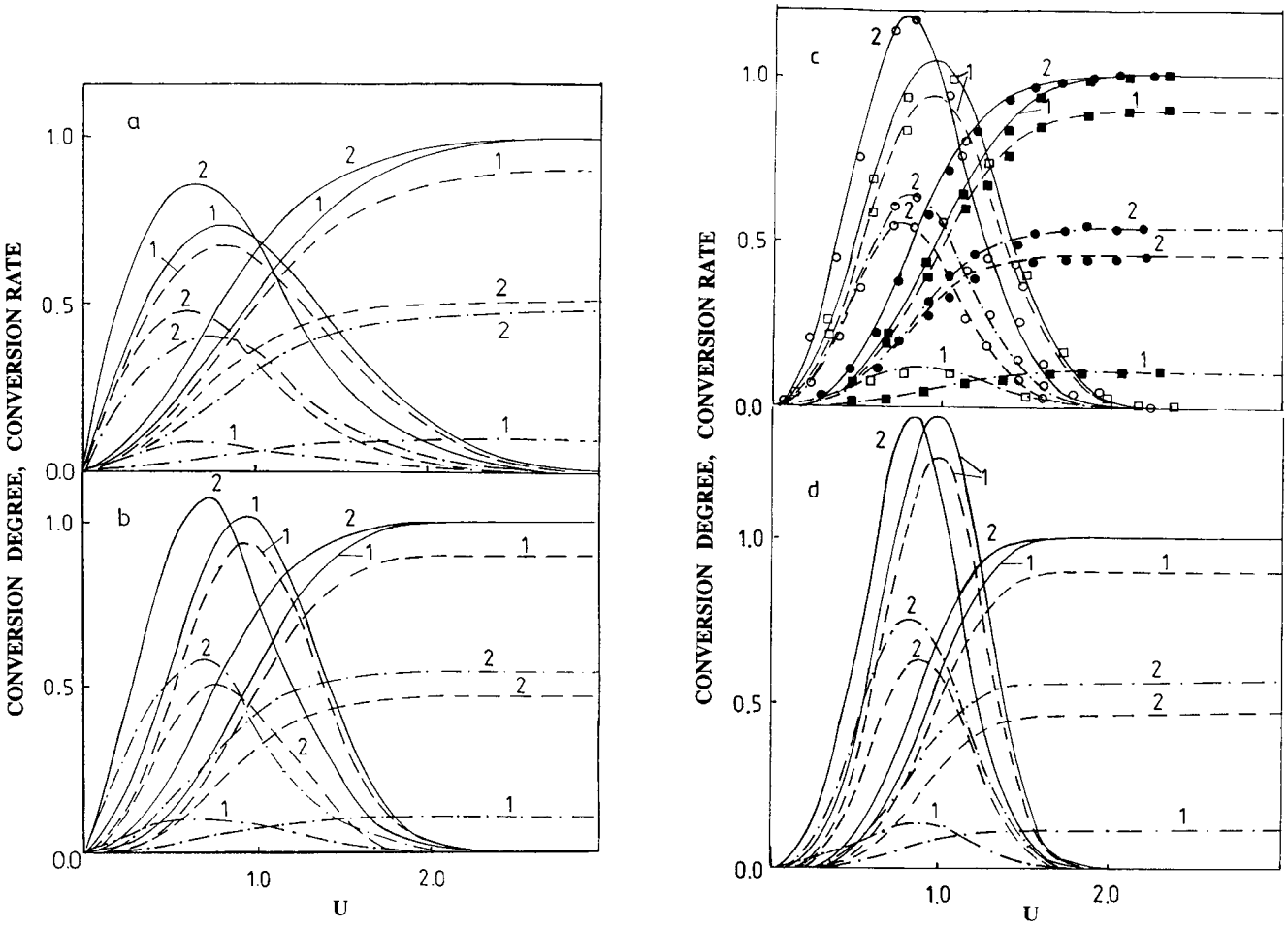

Fig. 3 Same as in Fig. 1 for samples of finite thickness with instantaneous nucleation at sample boundaries, for parameters B_1 (curves #1) and B_3 (curves #2) from Table 2; for spherulites nucleated inside a sample (– – –), for spherulites nucleated at sample boundaries (– · – · –) and for all spherulites together (——): a – 2D sample, instantaneous nucleation, b – 2D sample, isokinetic crystallization, c – 3D sample, instantaneous nucleation, d – 3D sample, isokinetic crystallization. Symbols denote the data from independent computer simulation

visible for $u > 2B_3$ due to the influence of the opposing sample boundary. The most pronounced changes are visible in the conversion degree in the middle of a sample, for $u > B_3$. In the absence of surface nucleation the conversion degree is significantly lower while for instantaneous nucleation at sample boundaries it is higher than for B_1 for the same u value. From the moment when spherulites nucleated at both sample boundaries reach the middle of a sample the conversion degree there increases rapidly and becomes even higher than at sample boundaries.

The distributions of distances from spherulites centers to spherulites interiors were calculated for all processes considered without and with additional nucleation at sample boundaries for $k = 1$ and respective values of parameter k_r. In Figs. 5a–6d the distributions of distances from spherulites centers to spherulites interiors are plotted as functions of variable v for a sample of finite thickness for the parameters C_1 and C_3 and for comparison for infinite samples [4]. The symbols denote the data from computer simulation. Similarly as for kinetics of crystallization, the points match well the curves depicting analytically obtained dependencies. The distance distributions for samples of limited thickness differ from those for infinite samples. In the absence of additional nucleation at sample boundaries the distributions are lower and broader. The effect increases with the decrease of sample thickness with respect to the average spherulite radius. The curves obtained for C_2 (not plotted in Figs. 5a–6d) are located always between those for C_1 and C_3. The additional instantaneous nucleation on sample boundaries causes an opposite effect; the distance distributions become narrower with maxima shifted towards smaller values of v. For smaller values of parameter C the effects are more pronounced. For cases with instantaneous nucleation at

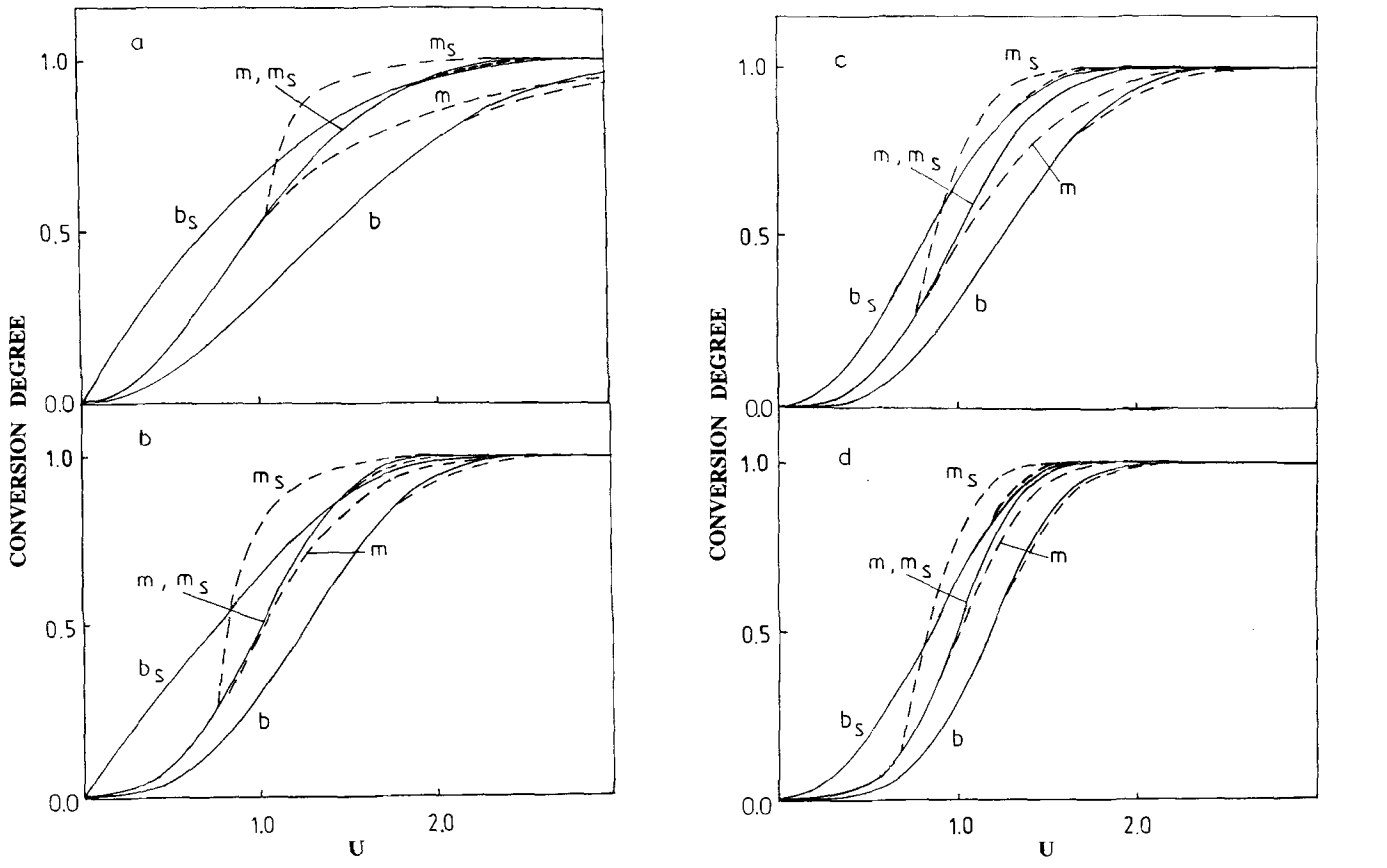

Fig. 4 The local conversion degrees as functions of a variable u for samples of finite thickness for parameters B_1 (——) and B_3 (– – –) at sample boundary (b) and in the middle of a sample (m). Subscript denotes processes with instantaneous nucleation at sample boundaries: a – 2D sample, instantaneous nucleation, b – 2D sample, isokinetic crystallization, c – 3D sample, instantaneous nucleation, d – 3D sample, isokinetic crystallization

sample boundaries also the component distance distributions are drawn: for spherulites nucleated at sample boundaries and for spherulites nucleated inside a sample. These distributions show the same range of distances within spherulites of both populations. Table 3 contains the comparison of numbers of spherulites per unit area or volume which were nucleated in infinite samples and inside samples of thickness of 40 units calculated for D and P values assumed for computer simulation. Table 3 contains also the radii of average spherulites. For processes with instantaneous nucleation at sample boundaries for $k = 1$ also the nucleation densities at sample boundaries and radii of average spherulites from that population are listed in Table 3. It follows that for isokinetic crystallization the finite thickness of samples leads to the decrease of average spherulite radius: up to 1% for B_1 and 3–5% for B_3. The instantaneous nucleation at sample boundaries causes decrease of the radius of spherulites nucleated inside a sample for both instantaneous nucleation and isokinetic crystallization: by 3–5% for B_1 and by 20–30% for B_3 (B_1 and B_3 are listed in Table 2). However, if spherulites nucleated at boundaries are taken into account, the decrease of radius of average spherulite is: for instantaneous nucleation by 11% and 8% for B_1, by 36% and 28% for B_3 in 2D and 3D samples, respectively, and for isokinetic crystallization: by 4% and 2% for B_1, by 18% and 10% for B_3 in 2D and 3D samples, respectively.

The conversion rate, $\hat{g}_{av}$, is plotted in Fig. 7a for the crystallization from instantaneous nuclei in a plate for B_1, B_2 and B_3 parameters, for two cases: rather weak and rather strong instantaneous nucleation at plate surfaces, characterized by k equal to 2 and 10, respectively. The component conversion rates for both spherulites populations: nucleated inside a plate, $\hat{g}_{iav}$, and at the surfaces, $\hat{g}_{sav}$, are drawn in Fig. 7b. The areas under $\hat{g}_{iav}$ and $\hat{g}_{sav}$ curves are equal to the contributions of respective spherulite populations to spherulitic structure. Additionally, the conversion rate for a plate with nucleation at surfaces only is also drawn. In this last case the values of nucleation density at surfaces and the variable u are the same as for

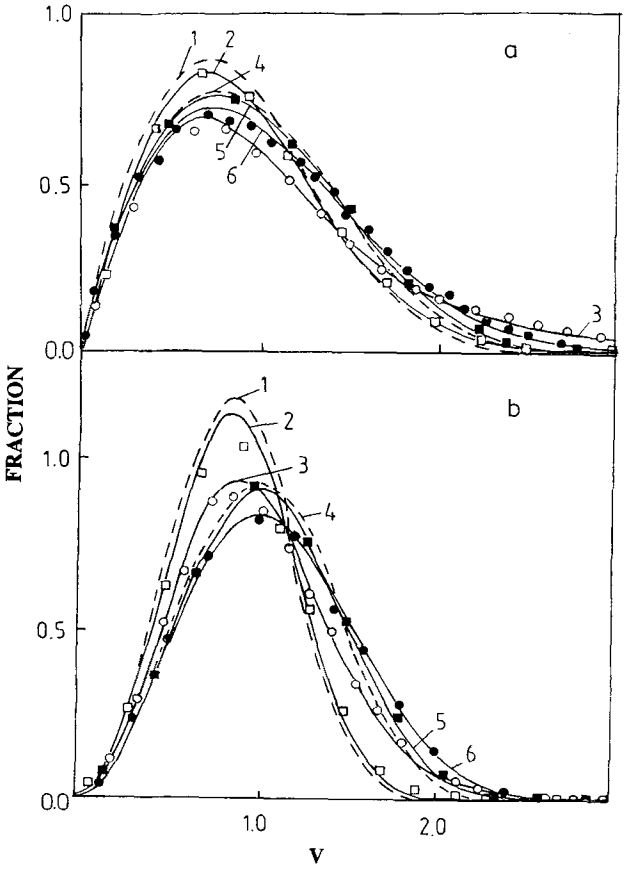

Fig. 5 The distributions of distances from spherulite centers to spherulite inner points as functions of a variable $v = r/r_s$, where r denotes the distance and r_s is the average spherulite radius, for instantaneous nucleation and for isokinetic crystallization for infinite samples (– – –), curves 1 and 4, and for samples of finite thickness (——) for parameters C_1 and C_3 from Table 2, curves 2 and 3 and curves 5 and 6, respectively. No nucleation at sample boundaries. Symbols denote the data from independent computer simulation. a – 2D sample, b – 3D sample

B_3 with $k = 2$ and $k = 10$. The examples of cross sections of computer-simulated crystallization spherulitic structures are shown in Fig. 8 for B_1 and B_3 for k equal to 2 and 10. For all values of parameter B considered stronger nucleation at plate surfaces causes changes in conversion rate curves: for B_1 and $k = 2$ the maximum lies between those for respective curves for $k = 1$ and $k = 0$ shown in

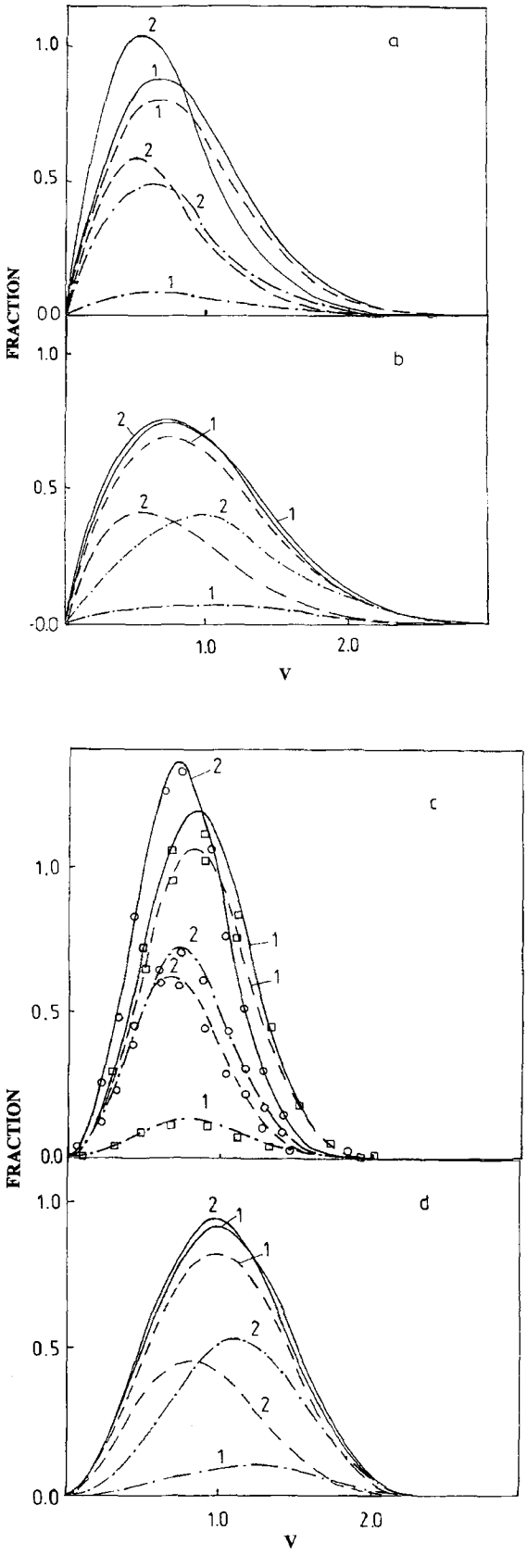

Fig. 6 Same as in Fig. 5 for samples of finite thickness with instantaneous nucleation at sample boundaries, for parameters C_1 (curves #1) and C_3 (curves #2): for spherulites nucleated inside a sample (– – –), for spherulites nucleated at sample boundaries (– · – · –) and for all spherulites together (——): a – 2D sample, instantaneous nucleation, b – 2D sample, isokinetic crystallization, c – 3D sample, instantaneous nucleation, d – 3D sample, isokinetic crystallization. Symbols denote the data from independent computer simulation

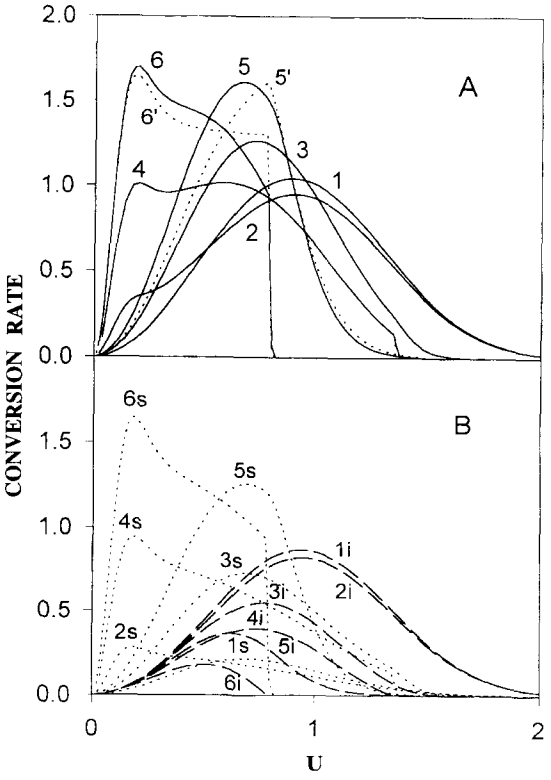

Fig. 7 The conversion rates in plates as functions of variable $u = r(0, t)/R_h$. a – the average conversion rates: curve 1 – B_1, $k = 2$, curve 2 – B_1, $k = 10$, curve 3 – B_2, $k = 2$, curve 4 – B_2, $k = 10$, curve 5 – B_3, $k = 2$, curve 6 – B_3, $k = 10$, curves 5′ and 6′ – the nucleation at sample surfaces only, with the density as for curves 5 and 6, respectively. b – the component average conversion rates, subscripts i and s denote the spherulites nucleated inside a plate and at plate surfaces, respectively. The numbers have the same meanings as in Fig. 7a

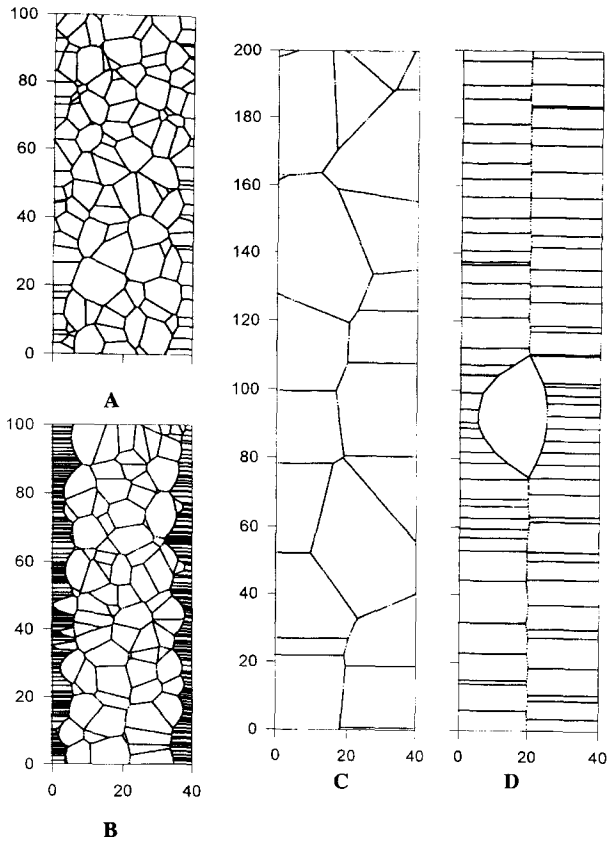

Fig. 8 The cross-sections of final spherulitic structures for weak and strong nucleation at surfaces for B parameter equal B_1 and B_3: a – B_1, $k = 2$, b – B_1, $k = 10$, c – B_3, $k = 2$, d – B_3, $k = 10$

Figs. 1c and 3c, but it is shifted towards smaller value of u, for $k = 10$ the lowering of the curve accompanied by the buildup of the shoulder for small u values is observed. Such effect during nonisothermal crystallization of polyamide 6-6 was observed and explained by Billon et al. [11] as the transformation of spherulites growing from sample surface from half-spheres to uniform front. For B_2 and B_3 the comparison of the plots of $\hat{g}_{av}$ for $k = 2$ with the respective plots for $k = 0$ and $k = 1$ depicted in Figs. 1c and 2c shows the narrowing of the curves, the increase of maximum values and the shift of position of maximum towards smaller value of u caused by enhancement of nucleation at surfaces. The increase of k to 10 results in the total change of shape of curve: the shoulder for small values of u observed for B_1 transforms into a separate maximum for B_2 while for B_3 it forms the main peak. Those transformations reflect the changes in conversion rates of two spherulites populations due to the changes of the relations between sample thickness, the density of nucleation inside a polymer and the density of nucleation at sample surfaces.

The respective component conversion rates of both spherulite populations, depicted in Fig. 7b, show that the increase of nucleation density at surfaces results in changes of the shape of $\hat{g}_{sav}$ accompanied by the formation of pronounced peak instead of rather flat maximum observed for weak nucleation at surfaces. The decrease of parameter B results in increased contribution of spherulites nucleated at surfaces to overall conversion rate. For B_2 and B_3 and $k = 10$ which corresponds to strong surface nucleation this contribution dominates, hence maximum of $\hat{g}_{sav}$ shows up in overall conversion rate. The analysis of the sequences of conversion rate curves for various values of k has shown that for all three values of parameter B the transcrystalline peak can be distinguished in the overall conversion rate for $k > 6$, hence for $D_s^{1/2} > 5D^{1/3}$. This is the condition necessary for the spherulites growing from the surface to form fronts before the significant impingement with spherulites nucleated inside a sample. For B_3 this transformation is accompanied by the sharp drop of $\hat{g}_{sav}$ and $\hat{g}_{av}$ when the spherulitic fronts growing from surfaces meet in the middle of the sample ($u = B$, shown here for B_3 and $k = 10$). However, even in this last case $\hat{g}_{sav}$ does not reach the

Colloid & Polymer Science, Vol. 275, No. 11 (1997)

constant level as it was suggested in Ref. [11], because even small number of spherulites nucleated inside a polymer disturbs the growing front of spherulites nucleated at sample boundaries. As it follows from the comparison of the plots in Fig. 7 the constant conversion rate can be achieved only in the absence of nucleation inside a polymer and if nucleation at surfaces is strong enough to enable the spherulites to form flat front before they reach the middle of a sample. It should be noted that the curves in Fig. 7 drawn as functions $v = uR_h/r_s$ would represent the distribution of distances from spherulite centers to their internal points, hence all remarks concerning the conversion rate curve are applicable also to those distance distributions.

Conclusions

For crystallization with instantaneous nucleation and for isokinetic crystallization there is a possibility to express analytically the relationships for the conversion degree and the rate of formation of spherulites interiors. The forms are characteristic for the type of crystallization process, and for the ratio of sample thickness to the extended spherulite radius at half-time of conversion of melt into spherulites. The distributions of distances from spherulite centers to spherulites interiors can also be written in the forms characteristic for the type of crystallization and for the ratio of sample thickness to the average spherulite radius. It should be mentioned here that the master curves characteristic for the type of the crystallization process can be obtained by dividing the extended radius at time t, $r(0, t)$, and the distance, r, by a distance characteristic for structure formation process or for final spherulitic structure in infinite sample. The characteristic distance could be, e.g. the extended radius at chosen moment of crystallization, the radius of average spherulite or its product by any constant.

Similar tendencies in the changes of kinetics of spherulite structure formation and in final spherulitic pattern were found in the cases considered in the paper for both two- and three-dimensional samples. It was shown that for the model processes considered the kinetics of spherulitic structure formation in samples of finite thickness differs from that in infinite samples. The correctness of the analytical approach was confirmed by the computer simulation of spherulite growth in nonisothermal conditions. The thinner samples with respect to spherulites radii, the more pronounced delay of conversion of melt into spherulite. It should be noted, however, that even in the case when the average conversion does not differ much from that for an infinite sample the crystallization is considerably slower at sample surfaces. These last conclusions are in the agreement with the results presented in refs. [8–10] for the kinetics of conversion in isothermal crystallization of samples of finite thickness. The influence of sample boundaries is also noticeable in the distributions of distances from spherulite centers to spherulite inner points. Thinning of samples results in broader distance distributions accompanied, in the case of isokinetic crystallization, by an increasing number of spherulites, thus by the decrease of average spherulite radius. For such sample with the thickness comparable to the average spherulite diameter, the number of spherulites is greater by 10% than that in infinite samples. However, during cooling of samples the influence of sample boundaries on crystallization kinetics and the final spherulitic structure could be modified to some extent by the temperature gradients resulting in lower temperature at the sample surfaces.

Even rare nucleation at sample boundaries accelerates the conversion which could become faster than that in infinite samples. It also results in narrowing of the distributions of distances and influences the number of spherulites nucleated inside a sample if nucleation in a polymer is prolonged in time. For instantaneous nucleation inside a sample these effects are enhanced by the stronger nucleation at surfaces, or by the decrease of nucleation inside a polymer, or by thinning of a sample. While rare nucleation at surfaces results in narrowing of the conversion rate curves accompanied by shifts of their maxima, the strong nucleation at sample surfaces, leading to crystalline front growing from surfaces, causes a significant change of shape of conversion rate curves: from the transcrystalline shoulder discussed in ref. [11] to the formation of a separate maximum which can convert into main peak of the curve. For instantaneous nucleation inside a polymer the influence of strong instantaneous nucleation on distribution of distances from spherulite centers to their internal points is the same as on the conversion rate curves.

Acknowledgement This research was supported primarily by the State Committee for Scientific Research, Poland, through the Centre of Molecular and Macromolecular Studies, PAS, under Grant 2 P303 101 04.

References

1. Piorkowska E (1997) Colloid Polym Sci 275:1035
2. Piorkowska E (1995) J Phys Chem 99:14007
3. Piorkowska E (1995) J Phys Chem 99: 14015

4. Piorkowska E (1995) J Phys Chem 99: 14024
5. Piorkowska E, Galeski A (1985) J Polym Sci, Polym Phys Ed 23:1273
6. Martuscelli E, Silvestre C, Abate G (1982) Polymer 23:229
7. Clark EJ, Hoffman JD (1984) Macromolecules 17:878
8. Billon N, Escleine JM, Haudin JM (1989) Colloid Polym Sci 267:668
9. Escleine JM, Monasse B, Wey E, Haudin JM (1984) Colloid Polym Sci 262:366
10. Billon N, Haudin JM (1989) Colloid Polym Sci 267:1064
11. Billon N, Magnet C, Haudin JM, Lefebvre D (1994) Colloid Polym Sci 272:633